IEEE/CSC & ESAS SUPERCONDUCTIVITY NEWS FORUM (global edition), October 2016.
ASC 2016 paper 2EOr1C-05. ASC Best Student Paper Contest (Electronics) Third Prize Winner.
DOI: 10.1109/TASC.2017.2661738

Study of X-ray Response of the TES X-ray Microcalorimeter for STEM

Haruka Muramatsu*, Tasuku Hayashi*, Keisei Maehisa*, Yuki Nakashima*,
Kazuhisa Mitsuda*, Noriko Y.Yamasaki*, Toru Hara† and Kyousuke Maehata‡
*Institute of Space and Astronautical Science
Japan Aerospace Exploration Agency(ISAS/JAXA), Kanagawa, Japan 252-5210
Email:muramatu@astro.isas.jaxa.jp
†National Institute for Materials Science (NIMS)
‡Department of Applied Quantum Physics and Nuclear Engineering, Kyusyu University

Abstract*—TES microcalorimeters show a nonlinear pulse-height-to-energy relation, reflecting their nonlinear resistance-to-temperature relation on the transition edge. In some of TES applications, such as energy dispersive X-ray spectroscopy (EDS), a wide energy range (e.g. 0.5-15 keV) and a good energy calibration (e.g. within a few eV) are required. We have studied the method to calibrate the nonlinear pulse-height-to-energy and to correct for it in the data analysis. We irradiated a TES microcalorimeter with three radio isotopes simultaneously to obtain continuum-free line spectra covering from 3.3 to 17.8 keV. X-ray lines from those isotopes are, respectively, a line complex containing fine structures and/or satellite lines, which can not be fully separated with TES microcalorimeters. Thus a special treatment is necessary. We first established a method to estimate the relation between PHA (Pulse Height Analyzed value by optimum filtering) and X-ray energy of the line complex precisely: we assumed that the relation can be approximated with a liner function, $PHA = aE + b$, locally in the narrow energy range containing one of the line complex, and determined a and b from the model fit of the PHA spectrum of the line complex. Then from the PHA-to-Energy relations of six line complexes, we determined a approximation formula which represents the global PH-to-energy relation. We then applied the global relation to convert PHA values of all pulses to energy equivalent value which we call PI (Pulse Invariant). We then fitted the PI spectra with the model function to check the consistency of energy. We have done these processes starting from two different forms of data; TES current as a function of time, and TES resistance as a function of time. The nonlinearity of PHA-to-energy was smaller for TES resistance pulses, and a better energy calibration is obtained. We found that the PI spectra obtained from TES current pulses reproduces the X-ray energies within ± 3 eV uncertainty, while the uncertainties becomes as larges as 10 eV for the PI spectra obtained from TES current pulses.

I. Introduction

High-energy X-ray spectrometers combined with electron microscopes are powerful tool for material micro analysis. Energy dispersive spectrometers using TES microcalorimeters are promising device. The advantage over wavelength dispersive spectrometers (WDS) is that TES microcalorimeters can cover wider energy ranges with almost constant FWHM energy resolution and potentially cover almost all elements from ^{5}Be to ^{92}U. We have been developing a TES X-ray microcalorimeter spectrometer for a Scanning Transmission Electron Microscope (STEM) [1]. The requirements for the spectrometers are (1) maximum counting rate of 5 kcps with a goal of 20 kcps, (2) an energy range of 0.5-15 keV, and (3) energy resolution of less than 10 eV (FWHM). In order to satisfy the counting requirement and to further fulfill the goal, we adopted an 8 $\times$8 format 64 pixel array, and we selected a relatively high TES transition temperature of 150 to 200 mK. We have not tested at a high counting rate environment yet, we consider the maximum counting requirement can be fulfilled with the TES array we have fabricated and tested so far from the fast decay time constant (50 μs) of an X-ray pulse [**?**]. We have also confirmed an energy resolution of 7 eV at 5.9 keV, although we have yet not confirmed the energy resolution at other energies.

When the resistance of the TES approaches its normal resistance, the sensitivity of TES as a thermometer reduces. As a consequence, when the incident X-ray phone energy is close to or more than ($E_{sat} \sim CT/\alpha$), the pulse height saturates and instead the pulse becomes longer. Here E, C and $\alpha = d\ln R/d\ln T$ are, respectively, the X-ray photon energy, the heat capacitance of the detector, and the TES sensitivity defined by the resistance-temperature ($R-T$) relation of the TES. As the consequence, the X-ray energy to pulse height relation becomes nonlinear. The nonlinearity degrade the energy resolution, because the optimum filtering used to determine the pulse height analyzed (PHA) value assumes linear response to energy[2]. Fixsen et al (2004)[3] proposed a modification of optimum filtering to recover energy resolution at high energies. On the other hand, Bandler et al. (2004) [4] partly corrected for the nonlinearity by converting the TES current signal as a function of time, $I(t)$, to resistance value, $R(t)$, before applying optimum filter. Since we need to determine the energies of unknown X-ray lines in EDS applications, we need precise energy-to-PHA calibration and nonlinear energy response can also be a problematic in calibration.

In this paper, we report our first attempt to calibrate the energy-to-PHA relation up to 17.8 keV. We will first show how we determine the the energy-to-PHA relation from line spectra which contain complex fine structures. We then determine the calibration curve and convert PHA to a value called PI (Pulse Invariant) in X-ray astronomy, and perform model fits to PI spectra. We find that the PI is better calibrated to energy when

IEEE/CSC & ESAS SUPERCONDUCTIVITY NEWS FORUM (global edition), October 2016.
ASC 2016 paper 2EOr1C-05. ASC Best Student Paper Contest (Electronics) Third Prize Winner.
DOI: 10.1109/TASC.2017.2661738

we apply optimum filter to $R(t)$ data than applying it to $I(t)$ data.

II. Energy to PHA relation in 3.3 – 17.8 keV

A. Experiment and event processing

We irradiated a TES microcalorimeter [5] with ^{41}Ca, ^{55}Fe, and ^{241}Am radio isotopes. The advantage of using radio isotopes than using electron excitation sources is that the spectrum is free from continuum. However, both radio isotopes and electron excitation sources have a disadvantage is that most of lines contain complex fine structures which cannot be fully resolved with our TES microcalorimeter. Thus we need relatively complicated data analysis to obtain the energy to PHA relation. We can avoid this problem by a monochromator. However, we will need a complicated set up between the X-ray source and the cryogenic Dewar. Another disadvantage is that the source is generally weak and we need long integration time to obtain statistically good spectra. Total integration time of the present experiment was 7 days, and we obtained 8205 events in K Kα line.

We first applied the optimum filter to TES current signal ($I(t)$ data) to determine the PHA of each events. Since we have corrected a largest number of events in K Kα from ^{41}Ca, and we created the pulse template for the optimum filter using the K Kα line. We then applied the template to each pulse events and obtained PHA values. We normalized the PHA values so that the PHA value at the peak of K Kα line in the PHA spectrum becomes 3313.8, which is the centroid energy of K Kα_1 in eV. In the PHA spectrum, we can clearly see following X-ray lines, K Kα, K Kβ, Mn Kα, Mn Kβ, Np L$_\alpha$ and Np Lβ. Np Lα and Np Lβ are, respectively, separated into 2 lines (Np Lα_1 and Np Lα_2) and 5 lines (Np Lβ_1 to Np Lβ_5. In addition, we can also see Np Lγ lines, 25 keV and 60 keV γ-ray lines. Since we are interested in the energy range bellow $\sim$ 15 keV for the STEM-EDS application and the total number of events is small for Np Lγ lines and above, we concentrate on X-ray lines below Np Lβ in this paper.

B. Model fits of PHA spectra

From the PHA spectrum, we would like to determine the PHA value which corresponds to a centroid energy of an X-ray line, e.g. K Kα_1. We would like to do this for the 6 X-ray line complexes, K Kα, K Kβ, Mn Kα, Mn Kβ, Np Lα_1 and Np Lβ_1. This is not a straightforward process, because, for example, K Kα_1 spectrum is strongly coupled with K Kα_2 spectrum and we need to model the fine structure of line to determine the PHA value of K Kα_1 precisely. We start from a line model function in the energy space

$$f(E) = \sum_{i=1}^{n} r_i L(E, E_{\mathrm{c},i}, \Gamma_i), \qquad (1)$$

where L and E are a Lorentzian function and photon energy, respectively. n is the number of fine-structure lines, and r_i, $E_{\mathrm{c},i}$ and Γ_i are, respectively, the relative intensity, the centroid energy, and the natural width of the i-th fine-structure line of the line complex. Values of most of those parameters are given in literature[6], [7].

TABLE I
Lines included in the model fits.

K Kα complex	Kα_1, Kα_2
K Kβ complex	Kβ_1, Kβ_3, K$\beta'^{(1)}_{1,3}$, K$\beta^{(2)}_5$
Mn K$_\alpha$ complex	K$\alpha_{1,1}$, K$\alpha_{1,2}$, K$\alpha_{1,3}$, K$\alpha_{1,4}$, K$\alpha_{1,5}$, K$\alpha_{2,1}$, K$\alpha_{2,2}$
Mn K$_\beta$ complex	Kβ_1, Kβ_3, K$\beta_{3,1}$
Np Lα, 1+sattelites	Lα_1, satelite1$^{(2)}$, satelite2$^{(2)}$, satelite3$^{(2)}$, satelite4$^{(2)}$
Np Lβ, 1 + Lβ, 3	Lβ_1, Kβ_2

(1) Natural width not found in literature.
(2) Natural width and intensity ratio not found in literature.

If we restrict model-fits to a narrow PHA range containing only one of the line complex, the PHA to energy relation can be approximated locally with a linear function; $PH = aE + b$. Then the model function in PHA space can be written as,

$$F(p) = N \sum_{i=1}^{n} \sum_{j} G(p - p_j, \sigma) r_i L(p_j, p_{\mathrm{c}}(E_i), \Gamma_{\mathrm{p}}(\Gamma_i)), \quad (2)$$

where p and $F(p)$ are, respectively, the PHA bin number and the PHA model spectrum. The centroid energies and widths are converted to PHA values (p_{c} and Γ_{p}) and the intrinsic line shapes are convolved with the line-spread function of the detector, which is described with a Gaussian function in PHA space. We performed six model fits for the line complexes in Tab. I. Although Np Lβ, 3 is separated from Lβ, 1 line by about 240 eV, we included this line in order to constrain the PHA to Energy relation. When values of r_i, $E_{\mathrm{c},i}$ and Γ_i of all fine structures are found in literature, the free parameters of the fits are, a, b, N (a normalization factor), and σ. If some of the line parameters are not known, we included them as free parameters.

In the fits, we maximized the likelihood assuming the Poisson statistics. From the residual of the fits (=data – model), we found that the PHA spectra contains an excess low PHA tail for K and Mn lines. This tail is likely a part of line spread function. Thus we added following term in the model function;

$$F_{\mathrm{tail}}(p) = u \sum_{i=1}^{n} r_i \exp\left(-\frac{p_i - p}{w}\right) \theta(p_i - p) \qquad (3)$$

where $\theta(p)$ is the Dirac's delta function, i.e. $\theta = 1$ for $p \geq 0$ and $\theta(p) = 0$ for $p < 0$. u and w are determined from the model fits. We did not add this tail component for Np Lα and Np Lβ.

In columns (a)–(c) of Tab. II, we show the best fit values of some free parameters, where Full Width Half Maximum (FWHM) was shown instead of the Gaussian σ. The statistical errors of fit parameters were estimated using so-called C statistics. We define $C = -2 \ln \mathcal{L}$, where $\mathcal{L}$ is the likelihood. It is known that $\Delta C = C_{\mathrm{true}} - C_{\mathrm{min}}$ follows χ^2 distribution with degrees of freedom which equals to the number of free parameters. All the errors quoted in the tables of this paper are single parameter errors at a 90% confidence level, which

IEEE/CSC & ESAS SUPERCONDUCTIVITY NEWS FORUM (global edition), October 2016.
ASC 2016 paper 2EOr1C-05. ASC Best Student Paper Contest (Electronics) Third Prize Winner.
DOI: 10.1109/TASC.2017.2661738

TABLE II
KEY PARAMETERS VALUES DETERMINED BY PHA SPECTRAL FITTINGS

		$I(t)$ pulse analysis			$R(t)$ pulse analysis		
Line	(Main peak (keV))	(a) FWHM (a.u.)	(b) a (a.u./eV)	(c) b (a.u.)	(d) FWHM (a.u.)	(e) a (a.u./eV)	(f) b (a.u.)
K Kα complex	(3.31380)	$4.31^{+0.18}_{-0.17}$	$1.0021^{+0.0001}_{-0.0049}$	$-5.8^{+0.1}_{-0.7}$	$4.58^{+0.20}_{-0.20}$	$1.00116^{+0.00004}_{-0.00030}$	$-2.1^{+1.75}_{-1.0}$
K Kβ complex	(3.59149)	$3.27^{+0.62}_{-0.65}$	$0.9956^{+0.0018}_{-0.0024}$	$-13.3^{+0.5}_{-0.2}$	$4.42^{+0.53}_{-0.44}$	$1.0066^{+0.0010}_{-0.0009}$	$-13.1^{+0.28}_{-0.3}$
Mn Kα complex	(5.89885)	$3.90^{+0.10}_{-0.25}$	$0.8000^{+0.00002}_{-0.00001}$	$844.6^{+0.2}_{-0.1}$	$5.33^{+0.21}_{-0.20}$	$1.0492^{+0.0039}_{-0.0075}$	$-166.3^{+0.32}_{-0.1}$
Mn Kβ complex	(6.49089)	$3.38^{+0.36}_{-0.42}$	$0.6249^{+0.0000}_{-0.0004}$	$1976.1^{+0.1}_{-0.6}$	$4.84^{+0.36}_{-0.70}$	$0.76305^{+0.0003}_{-0.00003}$	$1682.2^{+3.31}_{-2.5}$
Np Lα, 1+sattelites	(13.94426)	$6.90^{+2.09}_{-2.28}$	$0.5993^{+0.0012}_{-0.0013}$	$2052.7^{+0.6}_{-0.7}$	$8.27^{+4.54}_{-4.06}$	$1.0956^{+0.0179}_{-0.0036}$	$-2115.9^{+32.24}_{-2.1}$
Np Lβ, 1+Np Lβ, 3	(17.75020)	$5.25^{+1.37}_{-1.67}$	$0.32016^{+0.0001}_{-0.00003}$	$6161.4^{+0.8}_{-0.5}$	$11.80^{+2.94}_{-3.41}$	$0.5653^{+0.0014}_{-0.0001}$	$5604.0^{+51.49}_{-0.9}$

corresponds to $\Delta C = 2.7$ with all other free parameters re-optimized at the given value of the parameter of interest.

C. PHA to Energy relation

Then the PHA values corresponding to energy $E_{c,1}$ is determined by using the relation $PH = aE_{c,1} + b$ for each 6 fittings separately. The PHA values are plotted as a function of energy in Fig. 1 (a). From the figure, we find that the PH to energy relation is approximately linear up to $\sim$ Mn Kβ line, and show saturation for Np lines. We tried to find an analytic function which represents well the six PHA-to-E relation with a constraint that PHA=0 with $E = 0$. After several trials, we found that a polynomial function with order of four represents the experimental data points well. In Fig. 1 (a), we also show the best-fit polynomial function.

III. PI SPECTRA

Using the polynomial function, we can convert the PHA values of all the events of the experiment to a value which is close to energy. We call this value PI (Pulse invariant) following the tradition of X-ray astronomy. From the PI event list, we can create an energy spectrum in PI space and the six line complexes were fitted with a model function similar to the model in the previous section (Eq. (2) and (3)). Since in PI space, the energy response is supposed to be linearized, we set $b = 0$, but we set a free for each 6 lines separately. For Np Lβ line, we fitted the energy range containing Lβ_1 line and did not include Lβ_3. In columns (a) and (b) of Tab. III, we show the key parameters obtained from the fits, where we show the difference between the centroid PI and the model E of the main fine structure line, instead of the value of a. We also show the energy spectra and the best fit model of the six lines in PI space in Fig. 2.

IV. PULSE ANALYSIS USING TES RESISTANCE, $R(t)$

Nonlinearity in the TES microcalorimter energy response mainly arises from three different reasons: (1) temperature dependence of heat capacity of the detector, with which the temperature response against the incident X-ray photon energy becomes nonlinear, (2) nonlinear R-T relation of the TES, with which the resistance response to a temperature change becomes nonlinear, (3) deviation from a constant voltage in the TES bias. with which the TES current response to a resistance change becomes nonlinear. Bandler et al. (2004) [4] proposed

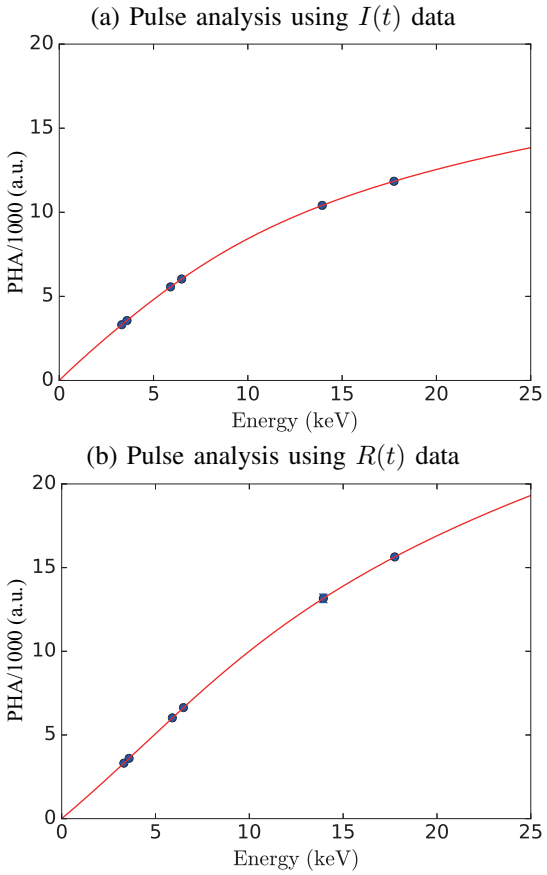

Fig. 1. Relation between pulse height (PHA) and X-ray energy for the six lines, K Kα, K Kβ, Mn Kα, Mn Kβ, Np Lα, and Np Lβ, determined by the model fits of lines in PHA spectra. The relation is approximated with a polynomial function of 4-th order. For the data points in panel (a), X-ray pulses in the TES current ($I(t)$) was processed with an optimum filter and the PHA of X-ray line was estimated by model fits. In panel (b) we applied optimum filter to the pulse record of the TES resistance, $R(t)$.

to correct for (3) before applying the optimum filter. In this section we follow this approach and see how the PHA-to-E calibration will be improved.

In the TES drive circuit, the TES and a shunt resister (R_s) are connected in parallel, and a constant bias current (I_b) is applied to them from a room temperature electronics. Then

IEEE/CSC & ESAS SUPERCONDUCTIVITY NEWS FORUM (global edition), October 2016.
ASC 2016 paper 2EOr1C-05. ASC Best Student Paper Contest (Electronics) Third Prize Winner.
DOI: 10.1109/TASC.2017.2661738

TABLE III
ENERGY CALIBRATION ACCURACY AND FWHM ENERGY RESOLUTIONS (EV) OF LINES OBTAINED WITH MODEL FITS OF THE PI SPECTRA

		$I(t)$ pulse analysis		$R(t)$ pulse analysis	
Line	(Main peak (keV))	(a) Main peak PI $-E$ (eV)	(b) FWHM (eV)	(c) Main peak PI $-E$ (eV)	(d) FWHM (eV)
K K_α complex	(3.3138)	$4.67^{+0.10}_{-0.20}$	$4.58^{+0.23}_{-0.18}$	$2.26^{+0.13}_{-0.06}$	$4.78^{+0.20}_{-0.21}$
K K_β complex	(3.59149)	$4.22^{+0.28}_{-0.71}$	$6.53^{+0.61}_{-0.60}$	$-1.04^{+0.30}_{-0.42}$	$5.84^{+0.56}_{-0.51}$
Mn K_α complex	(5.898853)	$2.40^{+0.21}_{-0.07}$	$4.58^{+0.20}_{-0.20}$	$-0.30^{+0.16}_{-0.09}$	$5.17^{+0.20}_{-0.19}$
Mn K_β complex	(6.49089)	$-0.56^{+0.22}_{-0.16}$	$3.93^{+0.53}_{-0.53}$	$1.27^{+0.23}_{-0.24}$	$3.93^{+0.56}_{-0.57}$
Np $L\alpha$, 1+sattelites	(13.94426)	$11.74^{+2.01}_{-1.24}$	$14.41^{+5.05}_{-4.03}$	$-0.56^{+1.74}_{-1.72}$	$16.13^{+6.25}_{-5.07}$
Np $L\beta$, 1	(17.7502)	$1.80^{+1.59}_{-1.60}$	$16.20^{+5.28}_{-5.09}$	$1.80^{+1.74}_{-1.79}$	$20.92^{+4.74}_{-6.65}$

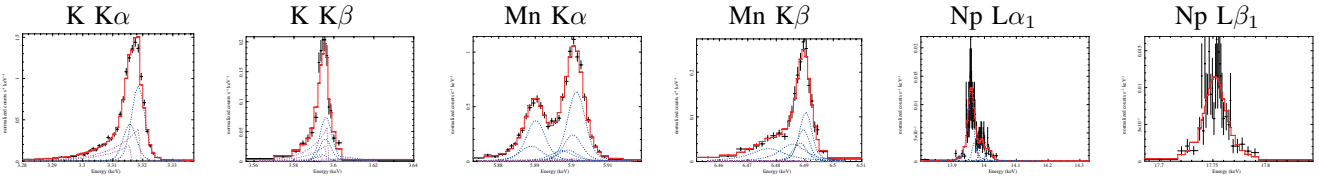

Fig. 2. Energy spectra of six line complexes and best fit models. The abscissa of spectra is PI which is converted from the PHA value (output of the optimum filtering of each X-ray pulses) using the calibration polynomial curve obtained from the PHA-to-Energy relation (Fig. 1). The components of the best fit model function are denoted with dotted lines; model components in Eq. (2) are denoted with blue dotted lines while those in Eq. (3) are with red doted lines.

the TES current at the bias point (I_0) is

$$I_0 = \frac{R_s}{R_s + R_0} I_b, \tag{4}$$

where R_0 is the resistance of the TES at the bias point. When the TES current changes from the bias point by ΔI, the change in the TES resistance is

$$\Delta R = -(R_0 + R_s)\frac{\Delta I}{I_0 + \Delta I} \tag{5}$$

We converted the TES current $I(t)$ to $R(t)$ and applied all the procedures described in the previous two sections to $R(t)$ pulse data. We show the results of model fits to PHA spectra in columns (d)-(e) of Tab. II, and the PHA-E relation in Fig. 1 (b). We fitted the relation with a 4-th order polynomial function and converted PHA to PI. The results of model fits to the PI spectra are summarized in columns (c) and (d) of Tab. III.

As we can see clearly from Fig. 1, the nonlinearity of the TES energy response was significantly reduced for the PHA spectra from $R(t)$ data. However, we could not confirm improvement of the energy resolution at high energies. The FWHM values of Np Lα and Lβ lines were respectivelly consistent to be same between the $I(t)$ and $R(t)$ spectra with in the 90% statisfftical errors. It is possible that the improvement of energy resolution is smaller than the 90% statistical errors. On the other hand, as far as we use a polynomial function of 4th order for PHA to PI conversion, we obtain better energy calibration for $R(t)$ spectra. We consider this is simply because the nonlinearity PHA to energy relation is smaller and thus the curve can be better represented with a simple analytical function. The fluctuation of the centroid energies obtained from the spectral fits was within ± 2 eV for $R(t)$ pulses, while it was as large as 12 eV for $I(t)$ pulses.

V. CONCLUSION

In this paper we have established the procedure to determine the PHA (Pulse Height Analyzer value) to energy relation of the TES X-ray microcalorimeter signal, and to apply it to convert PHA of individual events to PI (pulse invariant) values to obtain energy spectra. We have also show that if we convert TES current data to TES resistance data before applying the optimum filter to X-ray events, the nonlinearity of the PHA-to-energy relation is reduced and its calibration can be made more precise. In this paper, the method was applied to data taken with radio isotopes. However, the method can be applied to data obtained with electron excitation X-ray sources.

ACKNOWLEDGMENT

The authors would like to thank all the members of the JST STEM-TES project, which is supported by SENTAN, Japan Science and Technology Agency (JST).

REFERENCES

[1] K. Maehata, T. Hara, K. Mitsuda, M. Hidaka, K. Tanaka, Y. Yamanaka, J Low Temp Phys, DOI 10.1007/s10909-015-1361-3, 2015
[2] McCammon,D., in Cryogenic Particle Detection, Topics Appl. Phys. 99, 1-36, Ed. by Enss,C., Springer-Verlag, 2005
[3] Fixsen, D.J. et al., Journal of Physics Research A 520, 555-558, 2004)
[4] Bandler, S.R. et al., Journal of Physics Research A 520, 285-288, 2004
[5] H.Muramatsu, et al., Journal of Low Temperature Physics, 2016
[6] Zschornack G.H., in "Handbook of X-ray Data", Springer-Verlag Berlin Heidelberg, 1989, 2007
[7] Hölzer, G. et al., Physical Review Vol. 56, No. 6, pp. 4554 – 4568, 1997